HHS Public Access

Author manuscript

J Biol Rhythms. Author manuscript; available in PMC 2023 March 28.

Published in final edited form as:

J Biol Rhythms. 2020 December ; 35(6): 576–587. doi:10.1177/0748730420961214.

Light Has Diverse Spatiotemporal Molecular Changes in the Mouse Suprachiasmatic Nucleus

Phan Q. Duy[*,†,1], **Ruchi Komal**[*,1], **Melissa E. S. Richardson**[‡], **Katie S. Hahm**[*], **Diego C. Fernandez**[*], **Samer Hattar**[*,2]

[*]Section on Light and Circadian Rhythms, National Institute of Mental Health, National Institutes of Health, Bethesda, Maryland

[†]Medical Scientist Training Program, Yale University School of Medicine, New Haven, Connecticut

[‡]Department of Biology, Oakwood University, Huntsville, Alabama

Abstract

To be physiologically relevant, the period of the central circadian pacemaker, located in the suprachiasmatic nucleus (SCN), has to match the solar day in a process known as circadian photoentrainment. However, little is known about the spatiotemporal molecular changes that occur in the SCN in response to light. In this study, we sought to systematically characterize the circadian and light effects on activity-dependent markers of transcriptional (cFos), translational (pS6), and epigenetic (pH3) activities in the mouse SCN. To investigate circadian versus light influences on these molecular responses, we harvested brains from adult wild-type mice in darkness at different circadian times (CT) or from mice exposed to a 15-min light pulse at the middle of the subjective day (CT6, no phase shifts), early subjective night (CT14, large phase delays), or late subjective night (CT22, small phase advances). We found that cFos and pS6 exhibited rhythmic circadian expression in the SCN with distinct spatial rhythms, whereas pH3 expression was undetectable at all circadian phases. cFos rhythms were largely limited to the SCN shell, whereas pS6 rhythms encompassed the entire SCN. pH3, pS6, and cFos showed gating in response to light; however, we were surprised to find that the expression levels of these markers were not higher at phases when larger phase shifts are observed behaviorally (CT14 versus CT22). We then used animals lacking melanopsin (melanopsin knockout [MKO]), which show deficits in phase delays, to further investigate whether changes in these molecular markers correspond to behavioral phase shifts. Surprisingly, only pS6 showed deficits in MKOs at CT14. Therefore, our previous understanding of the molecular pathways that lead to circadian photoentrainment needs to be revised.

[2]To whom all correspondence should be addressed: Samer Hattar (NIH/NIMH) [E], Chief and Senior Investigator, Section on Light and Circadian Rhythms (SLCR), National Institute of Mental Health, John Edward Porter Neuroscience Research Center (Bldg 35), 35 Convent Drive, Room 2E-450, Bethesda, MD 20892; samer.hattar@nih.gov.

[1]These authors contributed equally to this work. Names were placed in alphabetical order.

CONFLICT OF INTEREST STATEMENT

The authors have no potential conflicts of interest with respect to the research, authorship, and/or publication of this article.

Supplementary material is available for this article online.

Keywords

light; phase shifts; circadian rhythms; suprachiasmatic nucleus; cFos; pS6; pH3; ipRGCs; retina; melanopsin

Organisms ranging from bacteria to humans have innate, endogenous 24-h biological rhythms that persist into constant conditions and can be entrained by the external light-dark cycle. These rhythms allow organisms to synchronize their activities with the predictable cycle of day and night, giving them a sense of time. In mammals, these daily rhythms are orchestrated by a central circadian pacemaker, located in the hypothalamus, the suprachiasmatic nucleus (SCN; Bass and Takahashi 2010). The SCN is synchronized to the environmental light-dark cycle via retinal photoreceptors. Light entrainment depends on a subset of intrinsically photosensitive retinal ganglion cells (ipRGCs) that express the photopigment, melanopsin, and that give rise to the retinal-hypothalamic tract, terminating in the SCN and certain other nonvisual brain areas (Provencio et al., 2000; Hattar et al., 2002, Hattar et al., 2006). The synchronization to the environmental light-dark cycle is based on a time-dependent responsiveness of the SCN to light, which is demonstrated by housing animals in constant darkness and subjecting them to discrete pulses of light. Light pulses presented during the early night induce phase delays of the rhythm, whereas the same light pulses presented at the end of the night induce phase advances. The same light pulses provided to animals in constant darkness during their subjective day cause no changes in the phase of the rhythm. The characteristic phase-dependent light responsiveness is a prerequisite for animals to entrain to the environmental cycle and is a common property of many organisms (Pittendrigh et al., 1984). Further, the magnitude of light-induced phase shifts of circadian locomotor activity rhythms also depends on the spectral composition, duration, and irradiance of the stimulus (Takahashi et al., 1984). Electrophysiological responses of melanopsin-positive RGCs have an action spectrum with a peak at 480 nm (Berson et al., 2002), coincident with the behavioral action spectrum for circadian photoentrainment. Attenuated phase delays in melanopsin knockout (MKO) mice were reported using a 15-min light pulse during early subjective night (Panda et al., 2002).

The SCN consists of approximately 20,000 neurons and is a heterogenous structure. At a simple level, the SCN can be divided into 2 major subregions based on neurochemical composition, connectivity, and spatial position. These subregions are typically referred to as the dorsomedial (also referred to as the dorsal or shell SCN) and ventrolateral (ventral or core SCN). The SCN receives most of its photic input from the retina directed toward its ventrolateral subregion, which has a connection in the SCN and outside the SCN to other brain regions controlling homeostatic functions (Kriegsfeld et al., 2004; Teclemariam-Mesbah et al., 1997; van Der Beek et al., 1997). The dorsomedial region is thought not to receive retinal input but to feature numerous direct and indirect projections to other hypothalamic nuclei controlling homeostatic functions and to the rest of the brain (Abrahamson and Moore 2001). Using genetic tracing techniques, it was shown that ipRGCs send projections to non–image-forming centers in the brain, including the SCN, which receives retinal input predominantly from M1 ipRGCs (Güler et al., 2008; Hattar et al., 2006; Welsh et al., 2010) and to a lesser extent from M2 ipRGCs (Welsh et al., 2010). The

molecules implicated in the photic signaling to the SCN are the excitatory neurotransmitter glutamate (Castel et al., 1993) and the neuropeptide pituitary adenylate cyclase activating protein (Hannibal et al., 1997). Their release leads to the activation of several signaling pathways and induction of clock genes and early immediate genes (Albrecht et al., 1997; Shearmen et al., 1997; Shigeyoshi et al., 1997; Morris et al.,1998; Crosio et al., 2000). Previous studies have reported that photic stimuli at the subjective night (when phase shifts occur), but not at the subjective day (when no phase shift occurs), generate diverse activity-dependent gene regulation pathways in SCN (Rusak et al., 1990; Cao et al., 2008), implicating these pathways as part of the signal transduction processes responsible for phase shift responses. The most studied of these pathways is the induction of cFos, an indirect transcriptional marker of neural activity (Earnest and Olschowka, 1993). Other studies have also correlated phase-shifting photic stimuli with increased phosphorylation of ribosomal protein S6 (pS6; Cao et al., 2008) and histone H3 protein (pH3; Crosio et al., 2000), phosphorylation events that are related to translational and epigenetic activities, respectively (Roux et al., 2007; Sawicka and Seiser, 2012). Although these light-induced molecular responses are often used as molecular proxies for circadian phase shifting (Shimomura et al., 1998; Cao et al., 2011; Fernandez et al., 2018; Hattar et al., 2003), the functional significance of these responses is not known. For instance, although studies have reported cFos induction only in response to phase-shifting light stimuli (Earnest and Olschowka 1993; Shimomura et al., 1998; Dkhissi-Benyahya et al., 2000), others have also reported that cFos is rhythmically expressed in the SCN in a circadian manner (Geusz et al., 1997; van der Veen et al., 2008). As mentioned earlier, the circadian system responds to light in a phase-dependent manner. However, it is not known whether the SCN also responds to light in a phase-dependent manner at the molecular level for phases that produce delays and advances. Furthermore, how these molecular responses are different in MKO animals that show attenuated phase delays compared with wild-type (WT) animals is currently unknown. Although it is believed that phase advances and phase delays occur through the same mechanisms (Watanabe et al., 2000), two studies in hamsters suggested that phase-advancing light pulses are correlated with more widespread expression of cFos in the SCN, particularly in the “shell” subdivision (Rea, 1992; Chambille et al., 1993), suggesting the involvement of different neuronal populations between phase advances and phase delays. However, studies in mice report similar patterns of cFos induction in the SCN by phase-delaying and phase-advancing light, and the increase in cFos expression tends to be limited to the core subdivision (Harmar et al., 2002; Hughes et al., 2004). Consequently, despite the well-known importance of light as a zeitgeber, the cellular and molecular mechanisms by which light cues are integrated with internal timekeeping mechanisms of the biological clock to synchronize circadian rhythms to the external light/dark cycle remain poorly understood.

In this study, we sought to systematically characterize the circadian and light effects on activity-dependent markers. We chose to cover three major aspects of these markers for transcriptional (cFos), translational (pS6), and epigenetic (pH3) activities in the mouse SCN. We also investigated circadian influences on these molecular responses. Independently, to investigate whether the SCN responds to light in a phase-dependent manner, we exposed mice to a 15-min light pulse at the middle of the subjective day when no phase shifts are observed (circadian time 6 [CT6]), early subjective night when large phase delays are

observed (CT14), or late subjective night when small phase advances are observed (CT22). Our studies reveal diverse interactions between the circadian clock and light input for these 3 molecular markers. They reveal that our understanding of the molecular pathways for light input that affect the circadian clock are primitive at best and provide the need to further investigate how the molecular changes in response to light are translated into changes in the phase of the circadian oscillator. Such studies are crucial for understanding the disruptive effects of light observed in shift work and transmeridian travel and probably for seasonal affective disorder as well.

MATERIALS AND METHODS

Animals

Two- to 3-month-old WT male mice of C57/B6 background (purchased from the Jackson Laboratory) were used to study the circadian and light effects on the SCN. To investigate the molecular changes in MKO animals, 2- to 3-month-old animals raised in the laboratory of the C57BL6/129 strain with their littermate WT controls were used. MKOs were produced as described in Hattar et al. (2002). Genotype was validated by Southern blotting and polymerase chain reaction (Hattar et al., 2002). All animals were handled in accordance with guidelines of the Animal Care and Use Committees of the National Institute of Mental Health. For the light pulse experiment, mice were first entrained to the 12:12 LD schedule, with an intensity of 380–400 lux (Philips daylight bulbs, ~1.4W/m^2 or ~320,000 photoisomerization rod^{-1} sec^{-1}) in light and 0 lux in darkness. After lights-off on the last day of the schedule, individual animals received either a single 15-min light pulse (the light source which is daylight bulbs with available spectrum so that the lux becomes relevant instead of meaningless; treated as the experimental group) or no light pulse (treated as dark control) either during their subjective day (CT6) or during their subjective nights (CT14/CT22). For each CT in the experimental group (light pulse) and control group (dark control), 13 to 15 and 10 to 12 animals were used, respectively.

Histological Preparations

Mice were deeply anesthetized using isoflurane. All mice were anesthetized under dim red light with their heads covered with a light-proof hood until they were perfused. After a 15-min light pulse at CT6/CT14/CT22, mice of the experimental group were perfused either after 15 min (i.e., CT6.50/CT14.50/CT 22.50) or 90 min (i.e., CT7.5/CT 15.5/CT 23.5) of the light pulse. Dark control mice did not receive a light pulse and were perfused at the same circadian times. The perfusion protocol consists of first perfusing the animal with approximately 5 mL of 1× phosphate-buffered saline (PBS) followed by approximately 40 mL of 4% paraformaldehyde (PFA) in PBS. Brains were removed and kept in 4% PFA overnight at 4 °C. Brains were then removed from PFA and kept in 30% sucrose in PBS for 48 h and then mounted in frozen OCT blocks. Brains were cryostat sectioned at a thickness of 35 μm and stored free floating in 0.05% PBS-azide and kept at 4 °C. Each animal yielded a total of 2 sets of brain sections (with each set containing 6 sections spanning the entire rostral-caudal SCN).

Immunofluorescence Staining

One set of SCN sections (containing 6 sections spanning the entire rostral-caudal SCN) from each animal was subjected to immunofluorescence staining, which was performed free-floating in 24-well plates. For pH3 and Ki67 staining, sections were first washed in 0.5% PBST. After 3 washes, the sections underwent antigen retrieval at 80 °C for 30 min in sodium citrate buffer (10 mM sodium citrate, 0.05% Tween 20, pH 6.0). Sections were cooled down at room temperature for approximately 20 min and then transferred to 0.5% PBST for washing. Sections were blocked in 10% bovine serum albumin (BSA; in 0.5% PBST) for 1 h and incubated in primary antibody diluted in 2.5% BSA (in 0.5% PBST); 1:1000 Phospho-Histone H3 rabbit mAb (Cell Signaling Technology, Danvers, MA) or 1:500 Ki67 rabbit mAb (Cell Signaling Technology). Primary incubation took 32 h at 4 °C. Sections were then washed in 0.5% PBST and incubated in secondary antibody diluted in 2.5% BSA (in 0.5% PBST), 1:500 donkey anti-rabbit Alexa Fluor 488 (Thermo Fisher) for 1 h. Sections were then washed in 0.5% PBST and incubated in DAPI solution 1:1000 in 0.5% PBST (Thermo Fisher) for 10 min at room temperature. Sections were finally washed in 0.5% PBST and mounted on slides by using Gold Antifade Mountant (Thermo Fisher, Waltham, MA).

For cFos and pS6 staining, after washing with 0.5% PBST, the sections were blocked in 10% BSA (in 0.5% PBST) for 1 h at room temperature and then incubated for 16 h at 4 °C in 1:2500 rabbit cFos mAb (Cell Signaling Technology). Sections were washed in 0.5% PBST and incubated in secondary antibody for 1 h, 1:500 donkey anti-rabbit Alexa Fluor 555 (Thermo Fisher). The sections were washed in 0.5% PBST and blocked with 1:500 rabbit immunoglobulin G diluted in 2.5% BSA (in 0.5% PBST) for 1 h at room temperature. Then the sections were incubated in primary rabbit mAb pS6 conjugated to Alexa Fluor 488 (Cell Signaling Technology), 1:750 diluted in 2.5% BSA (in 0.5% PBST) for 16 h at 4 °C. All steps were also followed for arginine vasopressin staining at 1:500 dilution for the primary antibody (rabbit mAb, Cell Signaling Technology).

After staining with the secondary antibody, sections were then washed in 0.5% PBST and incubated in DAPI solution 1:1000 in PBS (Thermo Fisher) for 20 min. Sections were finally washed in 0.5% PBST and mounted on a slide using Gold Antifade Mountant (Thermo Fisher).

RESULTS

We collected data from the harvested brains of adult WT C57/BL6 mice throughout various times of the circadian cycle: CT2, CT6, CT10, CT14, CT18, and CT22. We also measured light responses to a 15-min light pulse given at CT6, 14, and 22. We only chose one time (15 min) to carry out the light responses, because previous studies (Takahashi et al., 1984) showed that this duration is strong enough to induce phase shifts but short enough to prevent internal changes in the SCN that are related to intra-SCN signaling. To analyze the distribution of the molecular responses in the SCN and to show the spatiotemporal changes in a consistent fashion, we collected sections throughout the rostral-caudal extent of the SCN, which were marked by an unambiguous nuclear DAPI staining and were then delineated into the core and shell subdivisions based on arginine vasopressin expression, a

marker of the SCN shell (Fig. 1A). We are aware that our divisions of the shell and core of the SCN are arbitrary, but they will serve as posts for future studies since we are showing all SCN sections.

Circadian Analysis of cFos, pS6, and pH3 Expression in the SCN

We began by assessing circadian influences on cFos, the most studied light-inducible molecular marker (Rusak et al., 1990). This is partially due to the contradictory results in the literature regarding whether cFos expression is rhythmic (see van der Veen et al., 2008, for a detailed literature review). We found a strong circadian rhythm in cFos expression in the SCN across the rostral to caudal demarcations of the SCN (Fig. 1C). The circadian rhythm of cFos, however, was largely restricted to the shell subdivision of the SCN (Fig. 1C, D). This rhythm in cFos peaked during the middle of the subjective day (CT6) and reached its nadir during the middle of the subjective night (CT18). Next, we assessed the circadian influence on pS6, a marker of translation that has been shown to be correlated with neuronal activity and circadian phase shifting (Cao et al., 2008, 2011). Similar to cFos, we found that pS6 exhibited rhythmic expression in the SCN that peaked at CT6 (Fig. 1E, F). Thus far, both markers of neuronal activity and circadian phase shifting (cFos and pS6) have shown rhythmic expression under constant darkness. Consistent with previous observations (Crosio et al., 2000), we found an absence of pH3 staining in the SCN throughout all circadian phases under constant darkness (Fig. 1B).

Light-Induced Effects on cFos, pS6, and pH3 Expression in the SCN

There is a lack of spatial analyses of how light induces cFos in the SCN across the rostral to caudal aspects of the SCN. Consistent with previous studies (Rusak et al., 1990, Schwartz et al., 2000), cFos expression was not increased by light at CT6 (Fig. 2A, B). Despite high expression levels in the shell, light failed to induce any cFos in the core region (Fig. 2A, red circles). The overall density of cFos+ cells was similar between light at CT14 and light at CT22 (Fig. 2B). However, the greatest differences in the density of cFos+ cells were observed spatially, specifically, in the most rostral part of the SCN, which we considered to be part of the shell in our topographic analysis of cFos induction by light (Figs. 1A, 2A, B).

We then investigated the translational marker pS6. As expected, pS6 staining in the SCN was not increased by light at CT6 (Fig. 2C, D). However, we found a phase-dependent difference in the subjective night for pS6 staining. Specifically, the increases in the density of pS6+ cells at CT22 were much greater as compared with CT14 throughout the rostral-caudal levels of the SCN (Fig. 2C, D).

We and others have observed that phase-shifting light results in strong pH3 induction in the SCN and that light-induced pH3 responses are stymied in animals with impaired circadian phase shifting (Crosio et al., 2000). Light at CT6 did not result in pH3 induction in the SCN (Fig. 2E). Although the pH3 levels were not detected in constant darkness, light induced a robust level of pH3 at both CT14 and CT22 (Fig. 2E, F). Similar to pS6, but different from cFos, the density of pH3+ cells was significantly higher at CT22 as compared with CT14 throughout the rostral-caudal levels of the SCN (Fig. 2E, F).

Molecular Changes during Phase Delays versus Phase advances

To compare the effects of light on all 3 markers at CT14 and CT22, we plotted the data in comparison with dark controls for each molecular marker (Fig. 3). Light pulses at CT14 and CT22 generated a strong induction of cFos+ throughout the SCN (in both the core and shell; Fig. 3A). Despite the fact that light at CT14 induces much larger phase shifts in the phase of the circadian oscillator as compared with CT22, the cFos levels were similar (see also the section on MKO animals below). Furthermore, phase-advancing light stimuli showed a small but significant increase in cFos induction in the shell (Fig. 3A).

Similar to cFos, light pulses at CT14 and CT22 led to a strong induction of pS6+ throughout the SCN (in both the core and shell; Fig. 3B). Light at CT22 induced a greater density of pS6+ cells in the SCN as a whole as compared with light at CT14 (Fig. 3B), again despite smaller phase shifts at CT22. In addition, light at CT22 induced higher levels of pS6 in the shell regions as compared with light at CT14 (Fig. 3B), which led us to generate a model to explain the data.

Although both cFos and pS6 data showed differences between CT22 and CT14, the pH3 results were much more striking because of the lack of any staining in darkness (Fig. 3C). Light at CT22 showed a substantially greater density of pH3+ cells in the SCN as a whole as compared with light at CT14 (Fig. 3C). More detailed analysis revealed that the density of pH3+ cells was greater in both the core and shell subdivisions as well as in the rostral and medial parts of the SCN after light at CT22 as compared with light at CT14 (Fig. 3C). Importantly, given that pH3 is also a marker of mitotic cells, we also stained for Ki67, a marker of cell proliferation (Gerdes et al., 1983). We did not find any Ki67+ cells in the following phase-shifting light pulses (CT14 and CT22) or in the dark controls (Suppl. Fig. S1), indicating that light induction of pH3 in the SCN was not due to increased cell proliferation and more likely due to epigenetic changes. These observations show that unlike cFos and pS6, pH3 induction occurs only under settings of phase-shifting light stimuli and that this induction is much greater throughout the SCN following phase-advancing light as compared with phase-delaying light.

Investigating the Molecular Changes in MKO Animals

Previous studies have shown that MKO animals show attenuated phase delays in response to a 15-min light pulse (Panda et al., 2002). Thus, this would predict that the molecular changes in the marker genes would be attenuated in MKOs as compared with WTs. However, we observed attenuations in pS6 levels only in MKOs as compared with WT littermates (Fig. 4B [a-c]). The attenuation in pS6 was observed across the whole SCN, although it was only significant in the shell but not core region of the SCN. Both cFos and pH3 showed nearly similar changes in response to the light pulse (Fig. 4A [a-c], 4C [a-c]). We then investigated the molecular changes in these markers at CT22. Remarkably, all 3 markers showed a huge reduction in response to light for MKOs as compared with WT animals (Fig. 4A [d-f], 4B [d-f], 4C [d-f]). Future studies should investigate the phase-advancing effects of light on MKOs with regard to behavior as compared with WT animals to further understand this significant reduction in responses at CT22.

DISCUSSION

This study provides a systematic spatiotemporal characterization of the circadian and light effects on 3 markers of transcriptional, translational, and epigenetic activities. We confirmed several known facts about the light responses and provided new insights into the process. For example, we found that in all 3 markers, there are phase-dependent responses in the core of the SCN at CT14, when light can induce phase delays. This could explain why the field has assumed for so long that only VIP neurons receive light input from the retina. However, we also show that at CT22, there are clear light effects in the shell region of the SCN as well. In addition, we show that cFos has a circadian rhythm and find that it is confined predominantly to the shell region of the SCN.

We also revealed several novel findings. First, with the 3 markers, there was an increase in activation to light in the shell region at CT22 but not at CT14, indicating a possible inhibitory mechanism for blunting the phase-shift magnitude (Fig. 5; see also Romijn et al., 1996; Yamaguchi et al., 2013). Second, pS6 is a better marker than cFos for correlating the activity of the SCN, because it is high throughout the whole nucleus at CT6, when the firing rate of the SCN is highest. In contrast, cFos is low in the SCN core, where the activity is high. Third, pH3 provides the clearest light-dependent function in the SCN, because it is not observed in constant dark conditions. In addition, based on the results from the MKO animals, we predict that MKOs will have major deficits in phase advancing the clock.

cFos and pS6 exhibit strong rhythmic expression in the SCN under constant darkness, with the cFos confined to the shell region, whereas pH3 expression was induced only by phase-shifting light. Thus, among the markers we examined, we suggest that pH3 is an ideal marker for strictly studying the external effects of light on the SCN. Although cFos is the most commonly used molecular correlate for phase shifting, its rhythmic expression in the SCN shell that peaks during the middle of the day (when light produces no phase shift) suggests that cFos may also be a molecular marker for an internal gating mechanism in the SCN that limits the phase-shift responses (Schwartz et al., 1996). While pS6 expression is also rhythmic in the SCN, its expression is the highest in the entire SCN at CT6 (whereas cFos expression is limited to the shell), which correlates with previous observations that SCN neural activity peaks during the subjective day (Schaap et al., 2003; Kuhlman and McMahon 2006; Ko et al., 2009). Thus, we suggest that pS6 may be a molecular marker for neural activity. Our suggestion that different molecular markers reflect different properties of the clock (cFos for gating, pS6 for neural activity, and pH3 for external light effects) provides a new idea for understanding how light and the circadian clock interact to drive photoentrainment.

Our findings from WT and MKOs show that, in addition to the gating (represented by an asterisk [*] in our model; see Fig. 5) observed in the SCN between subjective day and night, the SCN unexpectedly responds to light at the subjective night also in a phase-dependent manner, as shown at CT14 and CT22. It is widely believed that phase advances and phase delays occur through the same mechanism, whereby advances and delays are determined by changes in the state variables of the circadian clockwork in response to light (Myers et al., 1996). Indeed, most studies show that both phase-advancing and phase-delaying photic

stimuli induce similar patterns (Kornhauser et al., 1990; Chambille et al., 1993; Masana et al., 1996). However, in our study, we found that phase-advancing light results in a wider distribution of pS6 and pH3 expression in the SCN, particularly in the shell, suggesting the potential involvement of separate neuronal populations in regulating phase advances and phase delays. Our study thus provides strong evidence that the same photic stimulus delivered at different time points of the subjective night leads to divergent molecular responses in the mouse SCN. Therefore, future investigations should specifically determine how the core and shell interact in coordinating circadian responses to phase-shifting light stimuli.

Supplementary Material

Refer to Web version on PubMed Central for supplementary material.

ACKNOWLEDGMENTS

We thank all members of the Hattar Lab for their guidance and support. The work was supported by the National Institute of Mental Health intramural program to S.H. (ZIAMH002964).

REFERENCES

Abrahamson EE and Moore RY (2001) Suprachiasmatic nucleus in the mouse: Retinal innervation, intrinsic organization and efferent projections. Brain Res 916:172–191. [PubMed: 11597605]

Albrecht U, Sun ZS, Eichele G, and Lee CC (1997) A differential response of two putative mammalian circadian regulators, mper1 and mper2, to light. Cell 91:1055–1064. [PubMed: 9428527]

Bass J and Takahashi JS (2010) Circadian integration of metabolism and energetics. Science 330:1349–1354. [PubMed: 21127246]

Berson DM, Dunn FA, and Takao M (2002) Phototransduction by retinal ganglion cells that set the circadian clock. Science 295:1070–1073. [PubMed: 11834835]

Cao R, Anderson FE, Jung YJ, Dziema H, and Obrietan K (2011) Circadian regulation of mammalian target of rapamycin signaling in the mouse suprachiasmatic nucleus. Neuroscience 181:79–88. [PubMed: 21382453]

Cao R, Lee B, Cho HY, Saklayen S, and Obrietan K (2008) Photic regulation of the mTOR signaling pathway in the suprachiasmatic circadian clock. Mol Cell Neurosci 38:312–324. [PubMed: 18468454]

Castel M, Belenky M, Cohen S, Ottersen OP, and Storm-Mathisen J (1993) Glutamate-like immunoreactivity in retinal terminals of the mouse suprachiasmatic nucleus. Eur J Neurosci 5:368–381. [PubMed: 7903187]

Chambille I, Doyle S, and Servière J (1993) Photic induction and circadian expression of Fos-like protein: immunohistochemical study in the retina and suprachiasmatic nuclei of hamster. Brain Res 612:138–150. [PubMed: 8330194]

Crosio C, Cermakian N, Allis CD, and Sassone-Corsi P (2000) Light induces chromatin modification in cells of the mammalian circadian clock. Nat Neurosci 3:1241–1247. [PubMed: 11100144]

Dkhissi-Benyahya O, Sicard B, and Cooper HM (2000) Effects of irradiance and stimulus duration on early gene expression (Fos) in the suprachiasmatic nucleus: temporal summation and reciprocity. J Neurosci 20:7790–7797. [PubMed: 11027243]

Earnest DJ and Olschowka JA (1993) Circadian regulation of c-fos expression in the suprachiasmatic pacemaker by light. J Biol Rhythms 8:S65–S71. [PubMed: 8274764]

Fernandez DC, Fogerson PM, Ospri LL, Thomsen MB, Layne RM, Severin D, Zhan J, Singer JH, Kirkwood A, Zhao H, et al. (2018) Light affects mood and learning through distinct retina-rain pathways. Cell 175:71–84. [PubMed: 30173913]

Gerdes J, Schwab U, Lemke H, and Stein H (1983) Production of a mouse monoclonal antibody reactive with a human nuclear antigen associated with cell proliferation. Int J Cancer 31:13–20. [PubMed: 6339421]

Geusz ME, Fletcher C, Block GD, Straume M, Copeland NG, Jenkins NA, Kay SA, and Day RN (1997) Long-term monitoring of circadian rhythms in c-fos gene expression from suprachiasmatic nucleus cultures. Curr Biol 7:758–766. [PubMed: 9368758]

Güler AD, Ecker JL, Lall GS, Haq S, Altimus CM, Liao HW, Barnard AR, Cahill H, Badea TC, Zhao H, et al. (2008) Melanopsin cells are the principal conduits for rod-cone input to non-image-forming vision. Nature 453:102–105. [PubMed: 18432195]

Hannibal J, Ding JM, Chen D, Fahrenkrug J, Larsen PJ, Gillette MU, and Mikkelsen JD (1997) Pituitary adenylate cyclase-activating peptide (PACAP) in the retinohypothalamic tract: a potential daytime regulator of the biological clock. J Neurosci 17:2637–2644. [PubMed: 9065523]

Harmar AJ, Marston HM, Shen SB, Spratt C, West KM, Sheward WJ, Morrison CF, Dorin JR, Piggins HD, Reubi JC, et al. (2002) The VPAC (2) receptor is essential for circadian function in the mouse suprachiasmatic nuclei. Cell 109:497–508. [PubMed: 12086606]

Hattar S, Liao HW, Takao M, Berson DM, and Yau KW (2002) Melanopsin-containing retinal ganglion cells: architecture, projections, and intrinsic photosensitivity. Science 295:1065–1070. [PubMed: 11834834]

Hattar S, Lucas RJ, Mrosovsky N, Thompson S, Douglas RH, Hankins MW, Lem J, Biel M, Hofmann F, Foster RG, et al. (2003) Melanopsin and rod-cone photoreceptive systems account for all major accessory visual functions in mice. Nature 424:76–81. [PubMed: 12808468]

Hattar S, Kumar M, Park A, Tong P, Tung J, Yau KW, and Berson DM (2006) Central projections of melanopsin-expressing retinal ganglion cells in the mouse. J Comp Neurol 497:326–349. [PubMed: 16736474]

Hughes AT, Fahey B, Cutler DJ, Coogan AN, and Piggins HD (2004) Aberrant gating of photic input to the suprachiasmatic circadian pacemaker of mice lacking the VPAC(2) receptor. J Neurosci 24:3522–3526. [PubMed: 15071099]

Ko G, Shi L, and Ko M (2009) Circadian regulation of ion channels and their functions. J Neurochem 110:1150–1169. [PubMed: 19549279]

Kornhauser JM, Nelson DE, Mayo KE, and Takahashi JS (1990) Photic and circadian regulation of c-fos gene expression in the hamster suprachiasmatic nucleus. Neuron 5:127–134. [PubMed: 2116813]

Kriegsfeld LJ, Leak RK, Yackulic CB, Lesauter J, and Silver R (2004) Organization of suprachiasmatic nucleus projections in Syrian hamsters (Mesocricetus auratus): an anterograde and retrograde analysis. J Comp Neurol 468:361–379. [PubMed: 14681931]

Kuhlman S and McMahon D (2006) Encoding the ins and outs of circadian pacemaking. J Biol Rhythms 21:470–481. [PubMed: 17107937]

Masana MI, Benloucif S, and Dubocovich ML (1996) Lightinduced c-fos mRNA expression in the suprachiasmatic nucleus and the retina of C3H/HeN mice. Mol Brain Res 42:193–201. [PubMed: 9013774]

Morris ME, Viswanathan N, Kuhlman S, Davis FC, and Weitz CJ (1998) A screen for genes induced in the suprachiasmatic nucleus by light. Science 279:1544–1547. [PubMed: 9488654]

Myers MP, Wager-Smith K, Rothenfluh-Hilfiker A, and Young MW (1996) Light-induced degradation of TIMELESS and entrainment of the *Drosophila* circadian clock. Science 271:1736–1740. [PubMed: 8596937]

Panda S, Sato TK, Castrucci AM, Rollag MD, DeGrip WJ, Hogenesch JB, Provencio I, and Kay SA (2002) Melanopsin (Opn4) requirement for normal lightinduced circadian phase shifting. Science 298:2213–2216. [PubMed: 12481141]

Provencio I, Rodriguez IR, Jiang G, Hayes WP, Moreira EF, and Rollag MD (2000) A novel human opsin in the inner retina. J Neurosci 20:600–605. [PubMed: 10632589]

Pittendrigh CS, Elliott J, and Takamura T (1984) The circadian component in photoperiodic induction. In: Porter R and Collins JM, editors. Photoperiodic regulation of insect and molluscan hormones. London: Pitman. p. 26–47.

Rea MA (1992) Different populations of cells in the suprachiasmatic nuclei express c-*fos* in association with light-induced phase delays and advances of the free-running activity rhythm in hamsters. Brain Res 579:107–112. [PubMed: 1623398]

Romijn HJ, Sluiter AA, Pool CW, Wortel J, and Buijs RM (1996) Differences in colocalization between Fos and PHI, GRP, VIP and VP in neurons of the rat suprachiasmatic nucleus after a light stimulus during the phase delay versus the phase advance period of the night. J Comp Neurol 372:1–8. [PubMed: 8841917]

Roux PP, Shahbazian D, Vu H, Holz MK, Cohen MS, Taunton J, Sonenberg N, and Blenis J (2007) RAS/ERK signaling promotes site-specific ribosomal protein S6 phosphorylation via RSK and stimulates cap-dependent translation. J Biol Chem 282:14056–14064. [PubMed: 17360704]

Rusak B, Robertson HA, Wisden W, and Hunt SP (1990) Light pulses that shift rhythms induce gene expression in the suprachiasmatic nucleus. Science 248:1237–1240. [PubMed: 2112267]

Sawicka A and Seiser C (2012) Histone H3 phosphorylation—a versatile chromatin modification for different occasions. Biochimie 94:2193–2201. [PubMed: 22564826]

Schaap J, Pennartz C, and Meijer J (2003) Electrophysiology of the circadian pacemaker in mammals. Chronobiol Int 20:171–188. [PubMed: 12723879]

Schwartz WJ, Carpino A Jr, de la Iglesia HO, Baler R, Klein DC, Nakabeppu Y, and Aronin N (2000) Differential regulation of fos family genes in the ventrolateral and dorsomedial subdivisions of the rat suprachiasmatic nucleus. Neuroscience 98:535–547. [PubMed: 10869847]

Schwartz WJ, Peters RV, Aronin N, Bennett R (1996) Unexpected cFos expression in the suprachiasmatic nucleus of mice entrained to a skeleton photoperiod. J Biol Rhythms 11:35–44. [PubMed: 8695890]

Shearman LP, Zylka MJ, Weaver DR, Kolakowski LF, and Reppert SM Jr (1997) Two period homologs: circadian expression and photic regulation in the suprachiasmatic nuclei. Neuron 19:1261–1269. [PubMed: 9427249]

Shigeyoshi Y, Taguchi K, Yamamoto S, Takekida S, Yan L, Tei H, Moriya T, Shibata S, Loros JJ, Dunlap JC, et al. (1997) Light-induced resetting of a mammalian circadian clock is associated with rapid induction of the mPer1 transcript. Cell 91:1043–1053. [PubMed: 9428526]

Shimomura K, Kornhauser JM, Wisor JP, Umezu T, Yamazaki S, Ihara NL, Takahashi JS, and Menaker M (1998) Circadian behavior and plasticity of lightinduced c-fos expression in SCN of tau mutant hamsters. J Biol Rhythm 13:305–314.

Takahashi JS, DeCoursey PJ, Bauman L, and Menaker M (1984) Spectral sensitivity of a novel photoreceptive system mediating entrainment of mammalian circadian rhythms. Nature 308:186–188. [PubMed: 6700721]

Teclemariam-Mesbah R, Kalsbeek A, Pevet P, and Buijs RM (1997) Direct vasoactive intestinal polypeptide-containing projection from the suprachiasmatic nucleus to spinal projecting hypothalamic paraventricular neurons. Brain Res 748:71–76. [PubMed: 9067446]

van der Beek EM, Horvath TL, Wiegant VM, Van Den Hurk R, and Buijs RM (1997) Evidence for a direct neuronal pathway from the suprachiasmatic nucleus to the gonadotropin-releasing hormone system: combined tracing and light and electron microscopic immunocytochemical studies. J Comp Neurol 384:569–579. [PubMed: 9259490]

van der Veen DR, van der Pol-Meijer MM, Jansen K, Smeets M, van der Zee EA, and Gerkema MA (2008) Circadian rhythms of C-FOS expression in the suprachiasmatic nuclei of the common vole (Microtus arvalis). Chronobiol Int 25:481–499. [PubMed: 18622811]

Watanabe K, Vanecek J, and Yamaoka S (2000) In vitro entrainment of the circadian rhythm of vasopressinreleasing cells in suprachiasmatic nucleus by vasoactive intestinal polypeptide. Brain Res J 877:361–366.

Welsh DK, Takahashi JS, and Kay SA (2010) Suprachiasmatic nucleus: cell autonomy and network properties. Annu Rev Physiol 72:551–577. [PubMed: 20148688]

Yamaguchi Y, Toru S, Yasutaka M, Hiroshi K, Kazuki O, Yulin C, Jean-Michel F, Fumiyoshi Y, Naoki M, Jing Z, et al. (2013) Mice genetically deficient in vasopressin v1a and v1b receptors are resistant to jet lag. Science 342:85–90. [PubMed: 24092737]

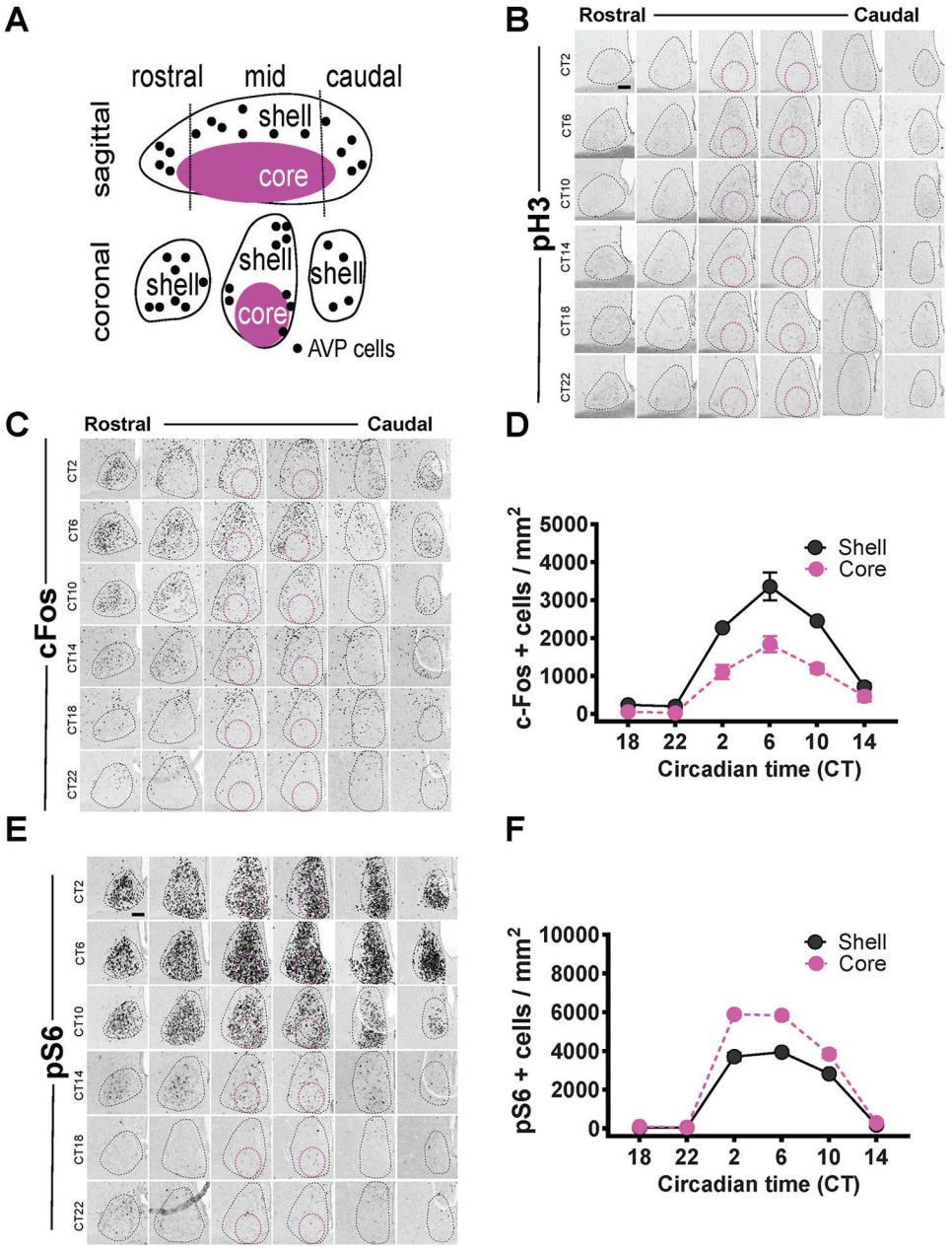

Figure 1.

Circadian analyses of pH3, cFos, and pS6 expression in the SCN. Delineation of the SCN into core and shell (A). Circadian expression of pH3 (B), cFos (C), and pS6 (E) in the SCN is outlined by the black dotted line, with the magenta circles showing the approximate core region. Quantification of the rhythms as mean ± SEM for cFos (D) row factor (circadian time), $F_{5,24} = 97.98$, $p < 0.0001$; column factor (core vs. shell), $F_{5,24} = 80.44$, $p < 0.0001$. Quantification of the rhythms as mean ± SEM for pS6 (F) row factor (circadian time), $F_{5,24} = 1040$, $p < 0.0001$; column factor (core vs. shell), $F_{5,24} = 212.7$, $p < 0.0001$. $n = 3$ mice per time point (24 animals total for both D and F). Some error bars are not visible because they are within the symbol in the plot. Scale bar: 94 μm.

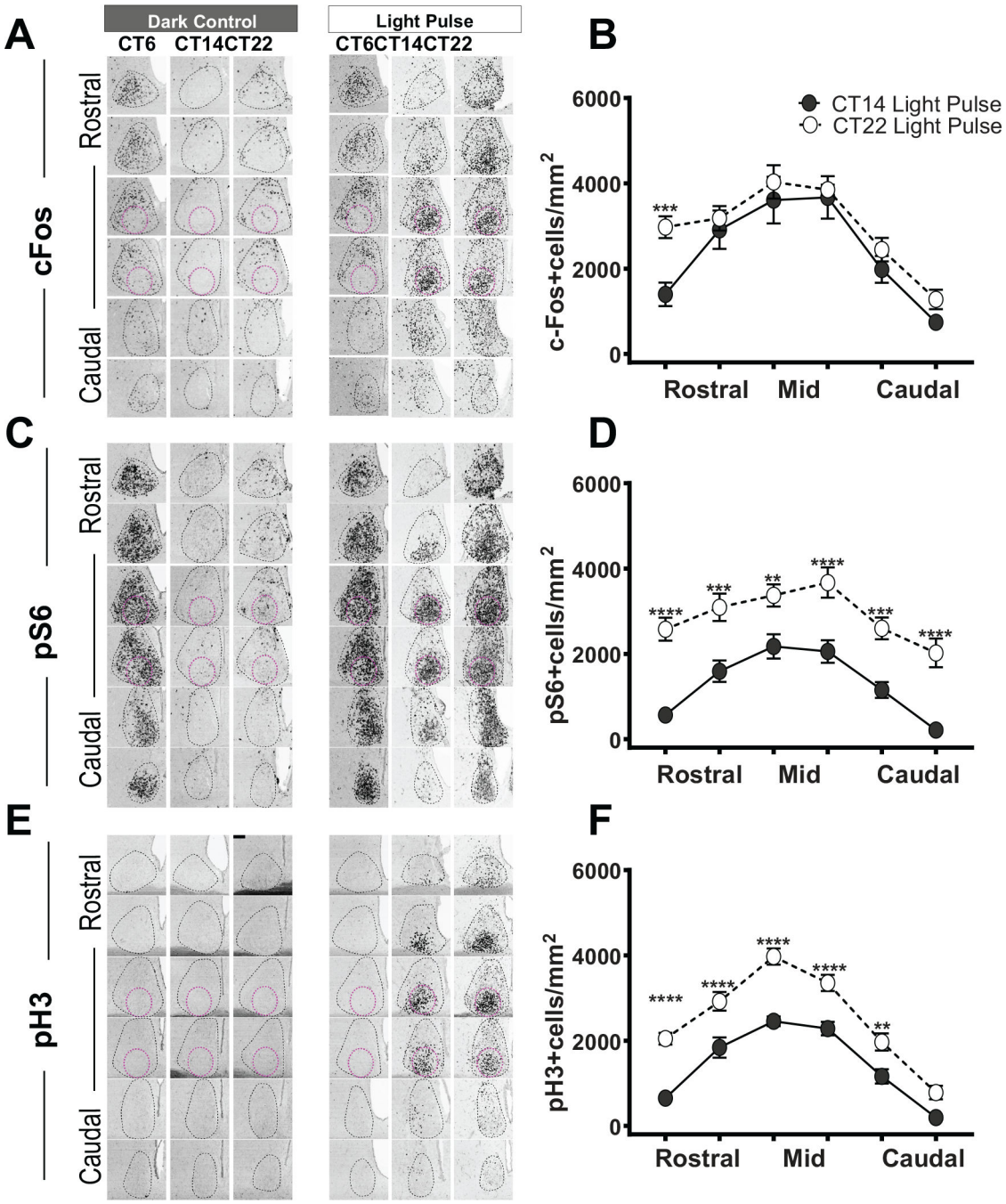

Figure 2.

Light-induced effects on cFos, pS6, and pH3 expression in the SCN. cFos (A), pS6 (C), and pH3 (E) expression in the SCN in darkness and following light pulses at CT6, CT14, or CT22. SCN is defined as in Figure 1. Quantification of cFos+ (B), pS6 (D), and ph3 (F) cell density (defined as the number of positive cells/area in mm^2) throughout the rostral-caudal levels of the SCN after light at CT14 (n = 7–9, each marker) or CT22 (n = 7–9, each marker). cFos (B) row factor (rostral to caudal), $F_{5,72} = 31.86$, $p < 0.0001$; column factor (CT14 light pulse vs. CT22 light pulse), $F_{1,72} = 13.50$, $p = 0.0005$. pS6 (D) row factor

(rostral to caudal), $F_{5,72} = 16.14$, $p < 0.0001$; column factor (CT14 light pulse vs. CT22 light pulse), $F_{1,72} = 129.2$, $p < 0.0001$. pH3 (F) row factor (rostral to caudal), $F_{5,96} = 74.81$, $p < 0.0001$; column factor (CT14 light pulse vs. CT22 light pulse), $F_{11,96} = 125.6$, $p < 0.0001$, 2-way analysis of variance. The asterisk (*) on the graph represents the difference between CT14 light pulse versus CT22 light pulse. Scale bar: 94 μm.

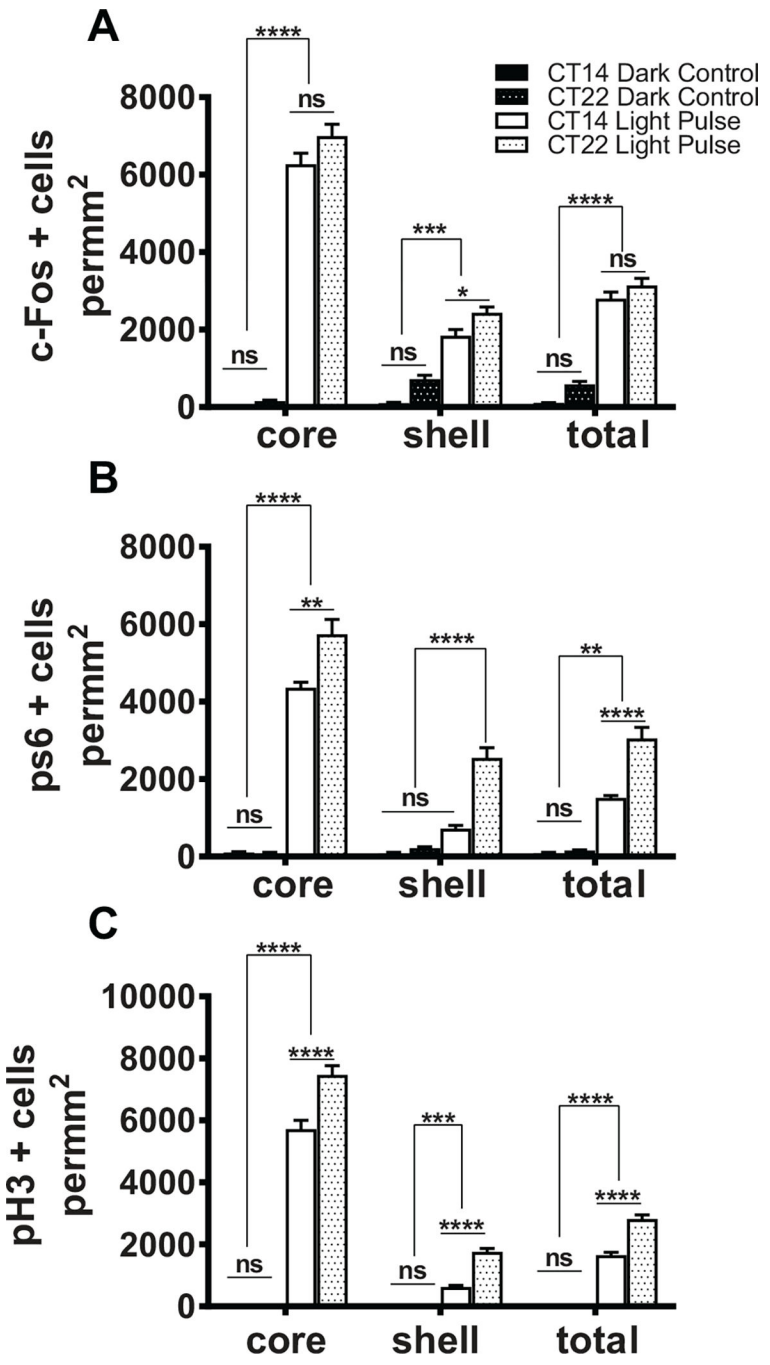

Figure 3.

Molecular changes during phase delays versus phase advances. Quantification of cFos+ cell density in the SCN core and shell in dark control ($n = 7$, each CT) and after a 15-min light pulse ($n = 7$, each CT) at CT14 or CT22 (a). ****$p < 0.0001$, 1-way analysis of variance (ANOVA), post hoc by Bonferroni's multiple comparisons test; ns indicates $p > 0.05$. Quantification of pS6+ cell density in the SCN core and shell in dark control ($n = 7$, each CT) and after a 15-min light pulse ($n = 7$, each CT) at CT14 or CT22 (B). ****$p < 0.0001$; ns indicates $p > 0.05$, 1-way ANOVA. Quantification of pH3+ cell density in the

SCN core and shell in dark control ($n = 7$, each CT) and after a 15-min light pulse ($n = 9$, each CT) at CT14 or CT22 (C). ****$p < 0.0001$; ns indicates $p > 0.05$, 1-way ANOVA.

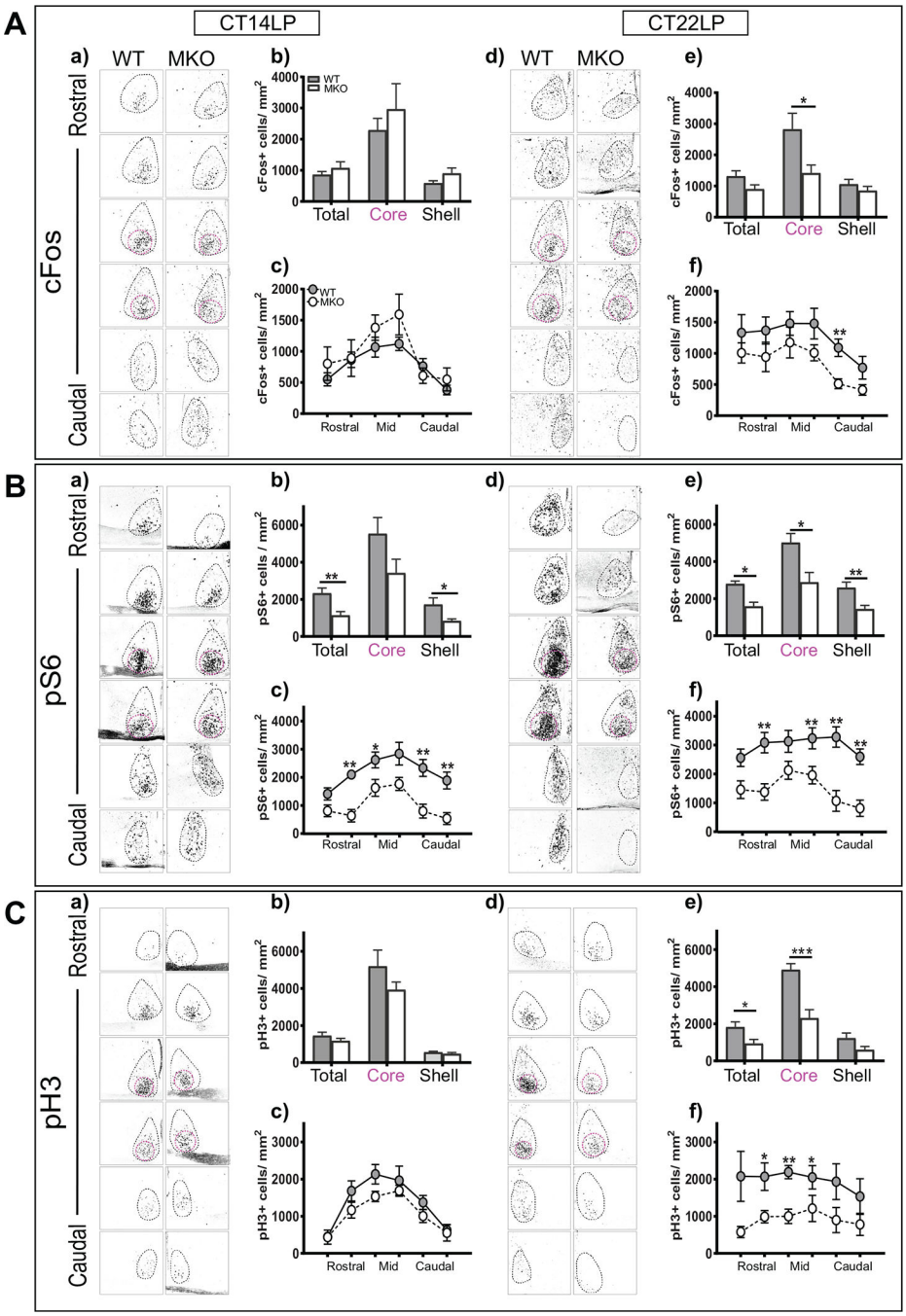

Figure 4.

Investigating the molecular changes in melanopsin knockout animals (MKOs). (a) SCN cFos expression following the light pulse at CT14. (b) Quantification of cFos+ cell density in the SCN core and shell after light at CT14. (c) Quantification of cFos+ cell density throughout rostral-caudal levels of the SCN after light at CT14. (d) SCN cFos expression following light pulse at CT22. (e) Quantification of cFos+ cell density in the SCN core and shell after light at CT22 (*$p < 0.05$, unpaired t test). (f) Quantification of cFos+ cell density throughout the rostral-caudal levels of the SCN after light at CT22 in MKos ($n = 6–7$) and wild-type (WT)

littermates ($n = 6$). Row factor (rostral to caudal), $F_{5,66} = 4.439$, $p = 0.0015$; column factor (WT vs. MKO), $F_{1,66} = 15.78$, $p = 0.0002$: 2-way analysis of variance (ANOVA) (A). (a) SCN pS6 expression following light pulse at CT14. (b) Quantification of pS6+ cell density in the SCN core and shell after light at CT14 (**$p < 0.05$, unpaired t test). (c) Quantification of pS6+ cell density throughout the rostral-caudal levels of the SCN after light at CT14. row factor (rostral to caudal), $F_{5,54} = 6.514$, $p < 0.0001$; column factor (WT vs. MKo), $F_{1,54} = 47.66$, $p < 0.0001$. Two-way ANOVA. (d) SCN pS6 expression following light pulse at CT22. (e) Quantification of pS6+ cell density in the SCN core and shell after light at CT22 (**$p < 0.05$, unpaired t test). (f) Quantification of pS6+ cell density throughout the rostral-caudal levels of the SCN after light at CT22 in MKos ($n = 6$–7) and WT littermates ($n = 6$). Row factor (rostral to caudal), $F_{5,66} = 2.382$, $p = 0477$; column factor (WT vs. MKO), $F_{1,66} = 65.93$, $p < 0.0001$, 2-way ANOVA (B). (a) SCN pH3 expression following light pulse at CT14. (b) Quantification of pH3+ cell density in the SCN core and shell after light at CT14. (c) Quantification of pH3+ cell density throughout the rostral-caudal levels of the SCN after light at CT14. (d) SCN pH3 expression following light pulse at CT22. (e) Quantification of pH3+ cell density in the SCN core and shell after light at CT22 (***$p <$ 0.05 unpaired t test). (f) Quantification of pH3+ cell density throughout the rostral-caudal levels of the SCN after light at CT22 in MKOs ($n = 7$) and WT littermates ($n = 7$). row factor (rostral to caudal), $F_{5,66} = 4.469$, $p = 00014$; column factor (WT vs. MKO), $F_{1,66}$ $= 37.03$, $p < 0.0001$, 2-way ANOVA (C). The asterisk (*) on the graph represents the difference between WT and MKO. Scale bar: 94 μm.

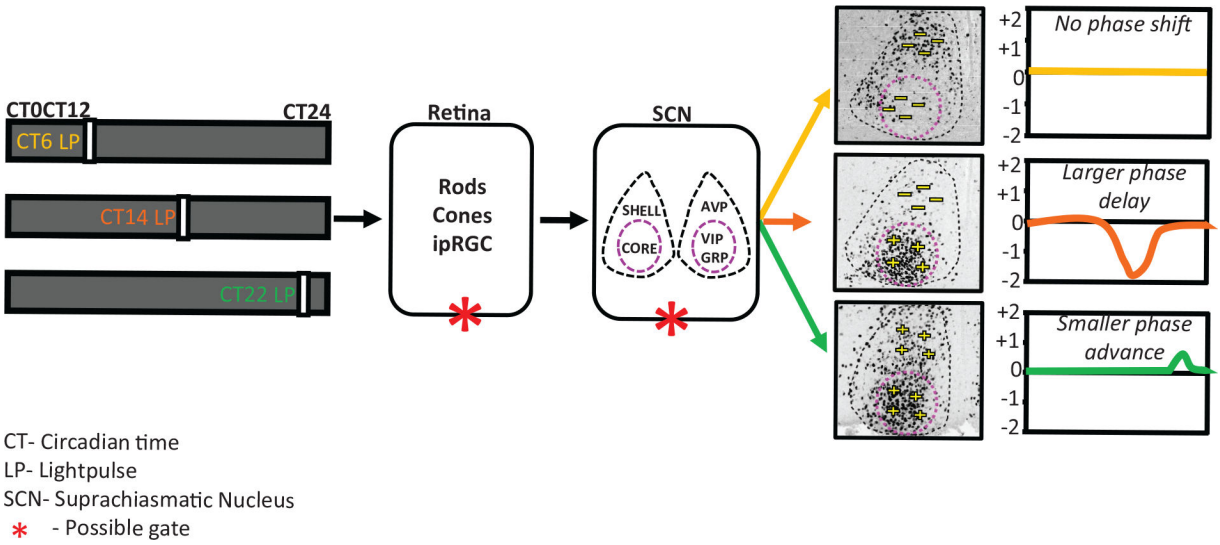

Figure 5.

Model representing light at a different time of the day differentially alters the SCN state dynamics and outputs. light input is received daily by specialized photoreceptor cells in the retina, intrinsically photosensitive retinal ganglion cells (ipRGCs), and transmitted via the retino-hypothalamic tract to the central clock located in the SCN, entraining it to the external light-dark cycle. The SCN is a bilateral structure and can be organized into 2 functionally distinct compartments: shell and core. The SCN shell contains a dense population of arginine vasopressin (AVP) neurons, and the SCN core contains vasoactive intestinal polypeptide (VIP) and gastrin-releasing peptide (GRP) neurons. Depending of the time at which the light pulse was given, the mice will show either no change or a phase shift of the activity rhythm after the pulse. There is also a clear phase-dependent response in the core and shell of the SCN at the phases when light can induce a phase shift. light pulse applied during the subjective day (CT6) causes no induction of cFos cells in the entire SCN, and no phase shift was observed. A light pulse applied at the beginning of the subjective night (CT14) causes a huge induction of cFos, but only in the core of the SCN, and larger phase delays were observed in activity. light pulses applied at the end of the subjective night (CT22) result in induction of cFos-positive cells in both the core and shell of the SCN and produce smaller phase advances. We propose that this light-signaling responsiveness is gate dependent and that the gating can be either at the retina level or within the SCN.